Supplementary Information (SI) for Materials Advances.

Supporting Information: Mechanically Driven Bacteria-Based Crack Detection

Ellen W. van Wijngaarden [a,b], Tyrone Chen [c], Ilana L. Brito [b,d], Nikolaos Bouklas [a,b,e], Andrea Giometto [b,f], and Meredith N. Silberstein [a,b,*]

[a] *Sibley School of Mechanical and Aerospace Engineering, Cornell University, Ithaca, NY*
[b] *Engineered Living Materials Institute, Cornell University, Ithaca, NY*
[c] Department of Material Science and Engineering, Cornell University, Ithaca, NY
[d] Meinig School of Biomedical Engineering, Cornell University, Ithaca, NY 14853, USA
[e] Pasteur Labs, Brooklyn, NY 11205, USA
[f] School of Civil and Environmental Engineering, Cornell University, Ithaca, NY 14853, USA
[*] Corresponding Author

E-mail: meredith.silberstein@cornell.edu
Phone: 607/255-5063

Contents

Supporting Figures

Supporting Tables

1 Supporting Figures

1.0 Spore Growth and Fluorescence

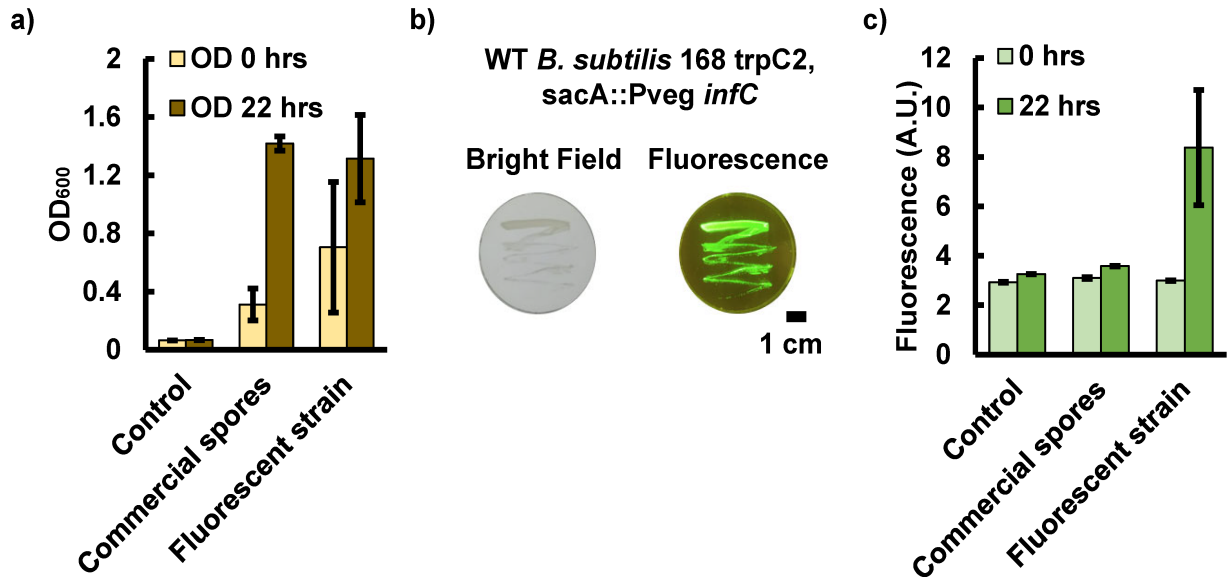

Figure S1: *B. subtilis* spores chosen for a) fast growth and b) strong constitutive fluorescent signal using the P*veg* promoter when grown on a LB agar gel plate or c) when grown in LB liquid media compared to non-fluorescent *B. subtilis* spores or commercially produced *B. subtilis* spores. Error bars report standard error of the mean (n=3).

2.0 Material Selection of Polymer Coating

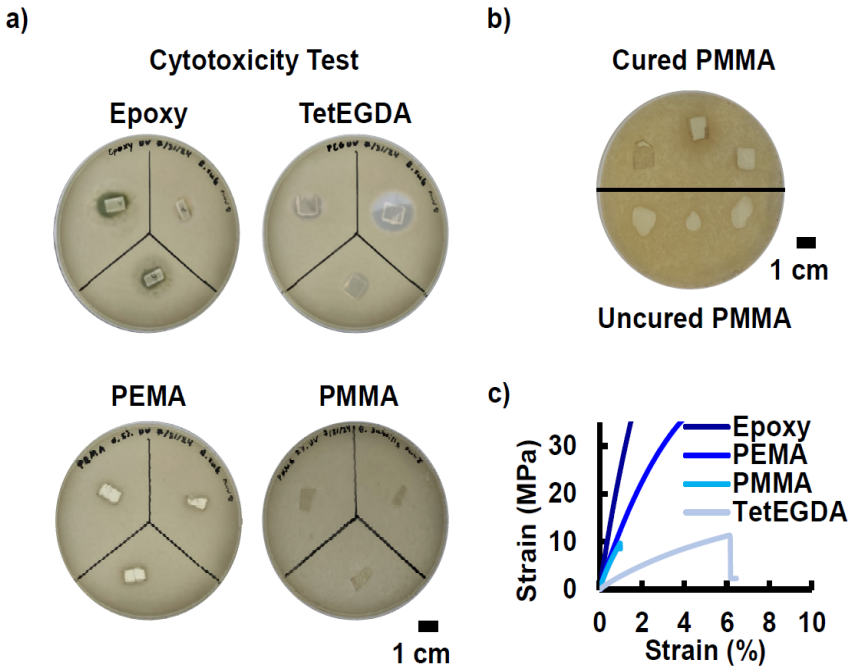

Figure S2: a) Cytotoxicity testing was performed by placing cured polymer blocks for each material candidate onto LB agar plates covered with spores. The plates were then incubated at 37°C and grown for 24 hours before the inhibition growth zones were measured. b) Cytotoxicity of cured PMMA blocks was compared to uncured MMA droplets to ensure that biocompatibility did not vary due to polymerization. c) Inset of Figure 1b for visualization of stress-strain curve of PMMA.

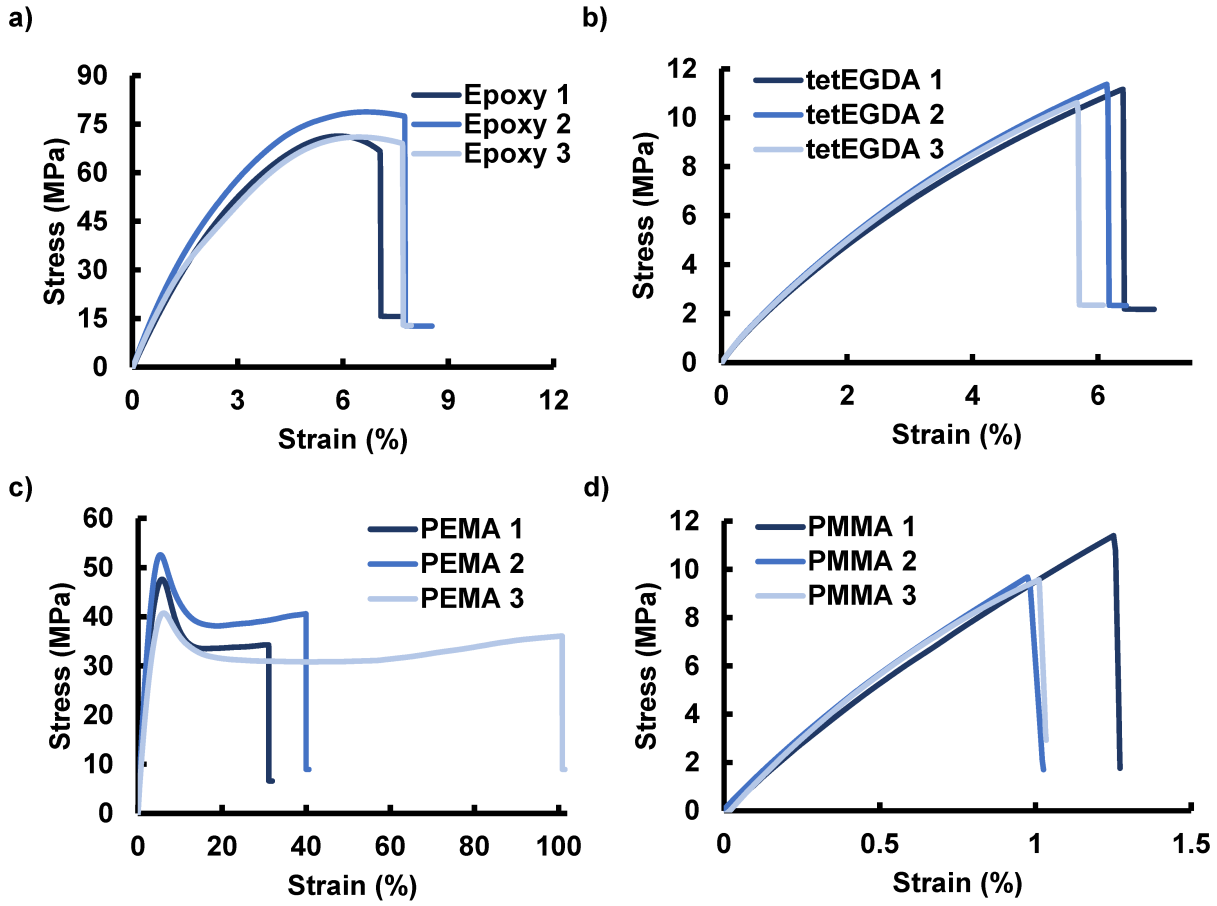

Figure S3: Uniaxial stress-strain behavior for a) Epoxy, b) tetEGDA, c) PEMA, and d) PMMA.

Table S1: Mechanical properties, Young's Modulus, ultimate tensile stress, and strain to failure, obtained from uniaxial tensile testing of potential coating materials.

Material	**Young's Modulus (GPa)**	**Ultimate Tensile Stress (MPa)**	**Strain to Failure (%)**
Epoxy 4500	2.22 ± 0.08	73.73 ± 4.39	7.51 ± 0.38
tetEGDA	0.22 ± 0.02	11.05 ± 0.39	6.06 ± 0.38
PEMA	1.44 ± 0.23	47.01 ± 5.95	57.79 ± 38.06
PMMA	1.18 ± 0.08	10.22 ± 1.03	1.08 ± 0.15

3.0 Mechanically Driven Crack Detection and Addition of Gel Layer

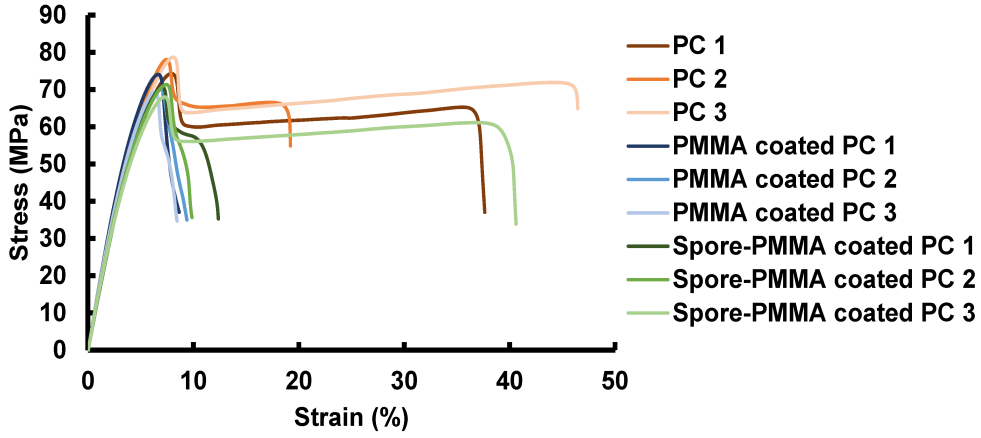

Figure S4: Uniaxial stress-strain behavior of PC, PMMA coated PC, and spore-PMMA coated PC dog bones.

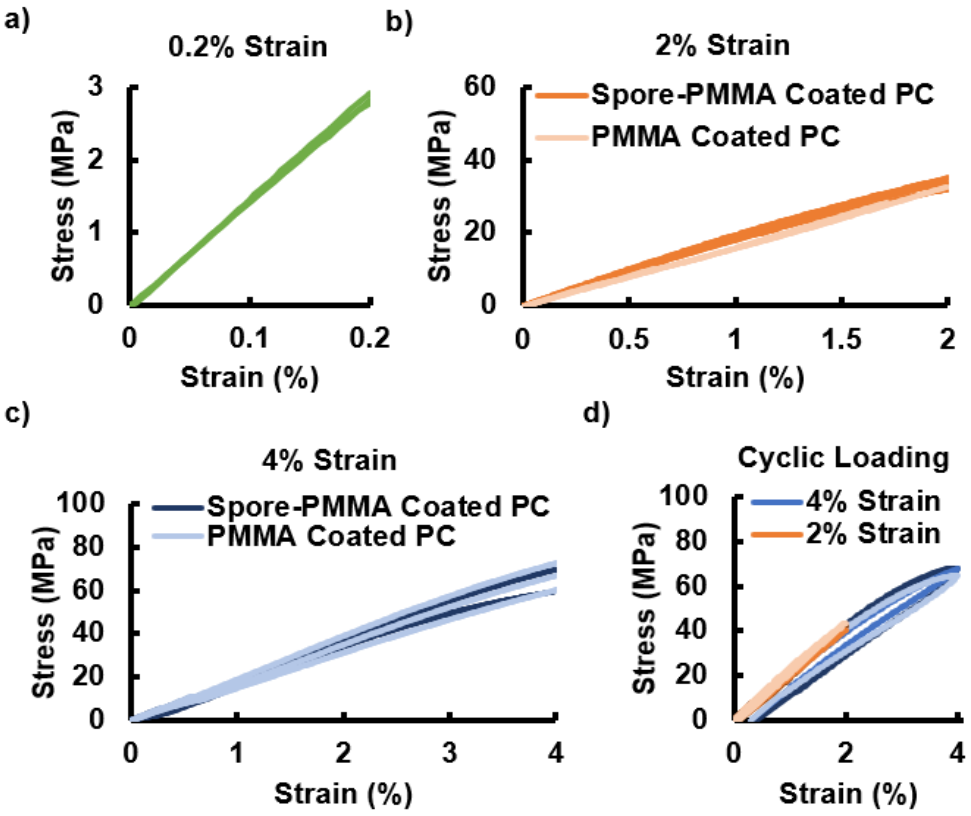

Figure S5: Stress-strain curves for the spore-PMMA coated polycarbonate samples for a) 0.2% strain, b) 2%, and c) 4% strain with and without spores embedded demonstrating similar stress-strain responses between spore and no spore samples. c) All cyclic trials for testing the amount of residual strain for 2% and 4% strain in the final spore coated samples.

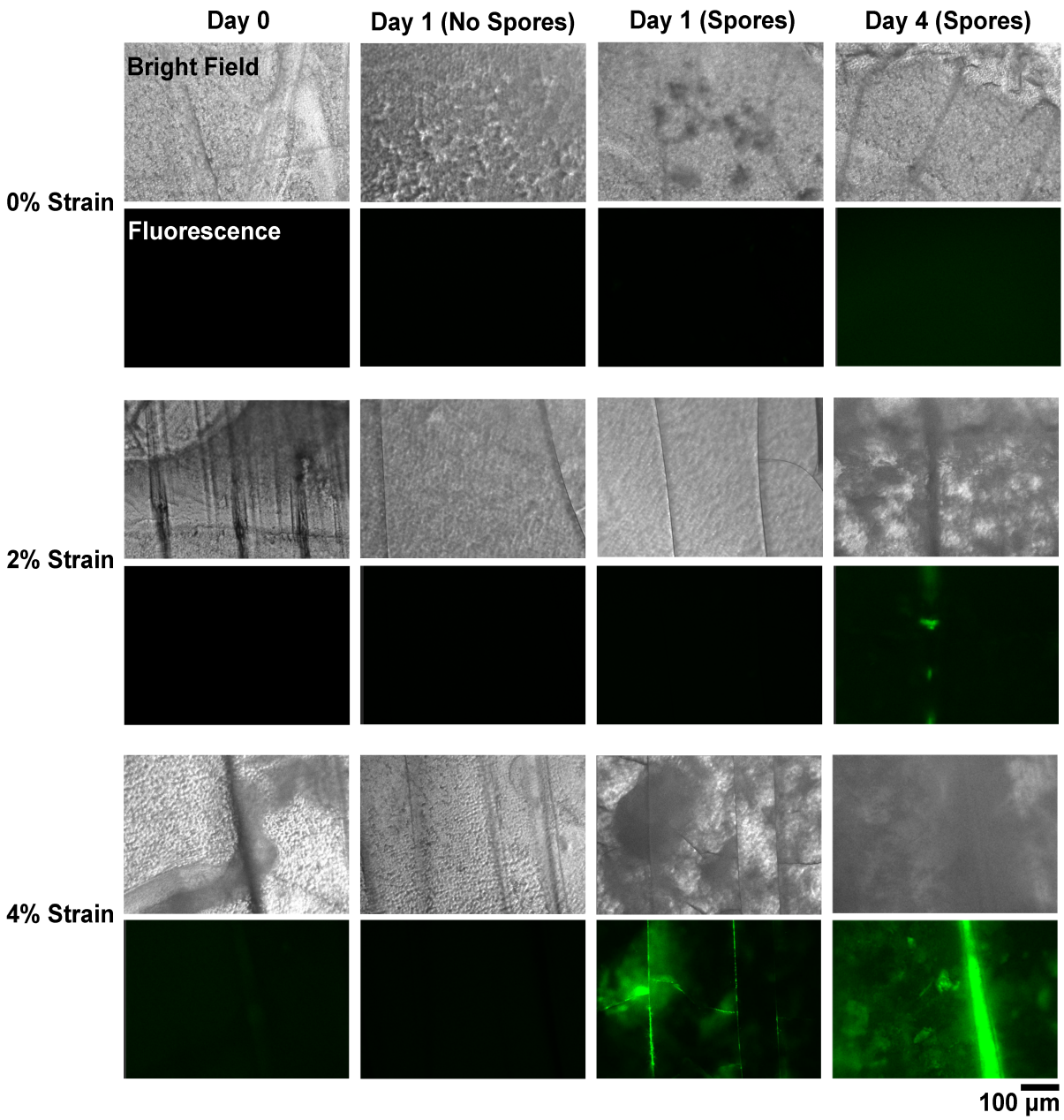

Figure S6: Bright field and fluorescent microscopy images of the cracks for spore-PMMA coated PC and PMMA coated PC dog bone samples.

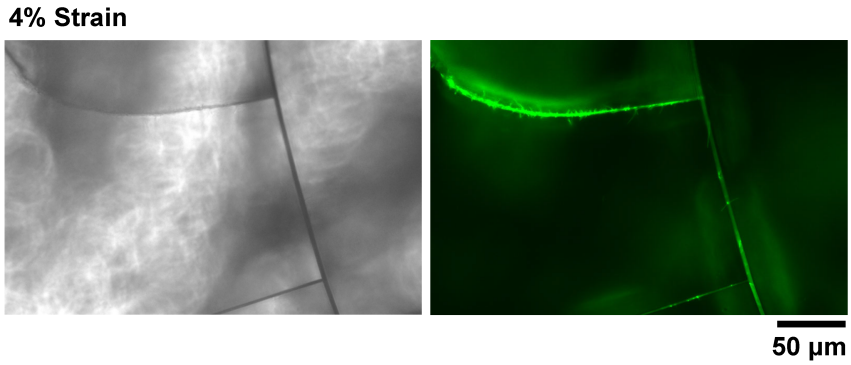

Figure S7: Bright Field and fluorescent images of a crack on a spore-PMMA coated polycarbonate sample that underwent 4% strain followed by 1 day of growth. The wispy fluorescent material on the crack outline are cells growing out of the cracks.

4.0 In Situ Detection of Localized Fatigue Damage: Nutrient Layer Selection and Design for Diffusion and Growth

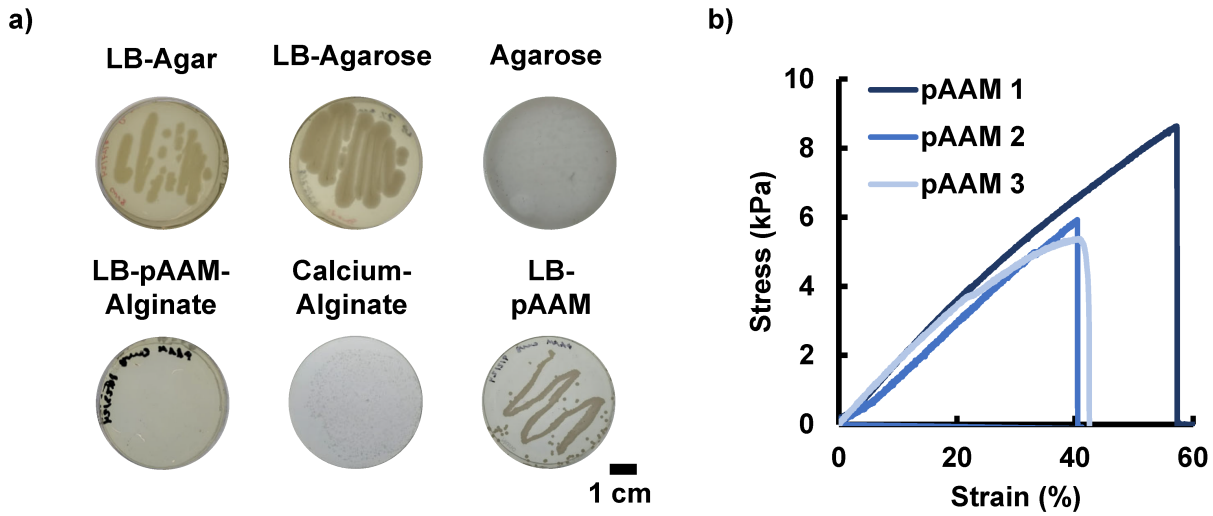

Figure S8: Nutrient gel layer candidates were tested for a) spore growth and b) mechanical properties. pAAM was the only gel with spore growth that has a sufficiently high strain to failure for the required coating and to be able to run tensile testing.

Diffusivity

The pAAM nutrient layer was selected based on biocompatibility and high strain to failure. The recipe was tuned to improve diffusivity of nutrients and growth by varying the crosslinker percentage, initiator concentration, and LB concentration. Diffusivity was determined by measuring the diffusion of safranin O dye through the different gel recipes to

measure the effect of crosslinking and initiator concentration. A hole, approximately 5 mm in diameter, was removed from the gel using a pipette tip. A volume of 10 μl of safranin O dye was added to the hole. Note that no dye was present above or below the gel surfaces. As the dye diffused outward from the center cylinder, images were taken at set time intervals. The dye radius was found by plotting the dye intensity profile in ImageJ and recording the full-width-half-maximum value as the dye diameter. The values for radius vs time were plotted and a linear fit was used to determine the slope. The diffusion coefficient was found using the slope of the line, following the equation $D = r^2/4t$ where r is the radius (cm), t is the time (s), and D is the diffusion coefficient (cm^2/s). The experiment was repeated for gels with varied crosslinker percentages (Figure S9a). Lower percentages had statistically significantly higher diffusivity.

Tensile Testing

Tensile testing was also conducted to ensure that the high stretch was maintained as the recipe was tuned (Figure S9b). Tensile testing methods followed those outlined in the main manuscript. Note that the gel with a crosslinker percentage of 0.01 was not stiff enough to grip for tensile testing and was therefore, ruled out. A crosslinker percentage of 0.04 was still mechanically robust enough to test, had a high ultimate strain (>20%), and a high diffusivity value. Therefore a crosslinker percentage of 0.04 was selected for additional tuning through varied nutrient and initiator concentration.

Microscopy for Improved Bacterial Growth

To measure bacterial growth on a gel plate, a custom built low-cost fluorescence microscope setup was designed following previous work by Shaefer et al (Figure S9c).[1] The in situ imaging setup was assembled using an optical table with quarter inch screws as the base (McMaster Carr, Elmhurst, IL). Four symmetrical threaded rods were placed equidistant from the four corners of the optical table acting as the structural support of the setup (McMaster Carr). Two layers of plexiglass (Art3d, Independence, MO) were mounted onto the rods to hold the sample and the color filter (Weindasi, China). The first plexiglass layer served as a sample holder and was secured using nuts and threaded rods. Nuts were placed above and below the plexiglass at each of the four threaded rods to ensure stability. This design allows for open space above the sample where the 525/50 nm filter was placed and held by the nuts placed above and below. A final wood layer was placed above the second layer of plexiglass with the same drilled hole configuration. This is used to hold a camera/ smartphone (iPhone, Apple, Cupertino, CA). Imaging was conducted using a blue light (WF-502B, Ultrafire, Chicago, IL) for excitation. The light source was placed one foot from the sample for uniform illumination. Imaging was conducted in a completely dark environment. These images were analyzed using ImageJ. The plate area was defined as the region of interest and the average fluorescence intensity was recorded.[2] Gel plates, with varied nutrient (Figure S9d) and TEMED initiator (Figure S9e) concentrations, were compared for fluorescence intensity due to cell growth. Significantly higher fluorescence was observed for 2x LB nutrient concentrations and for lower initiator concentrations. However a TEMED concentration of 0.5 μl/ml was not stiff enough to handle. Therefore a nutrient

concentration of 2x LB and a TEMED concentration of 1 μl/ml was used.

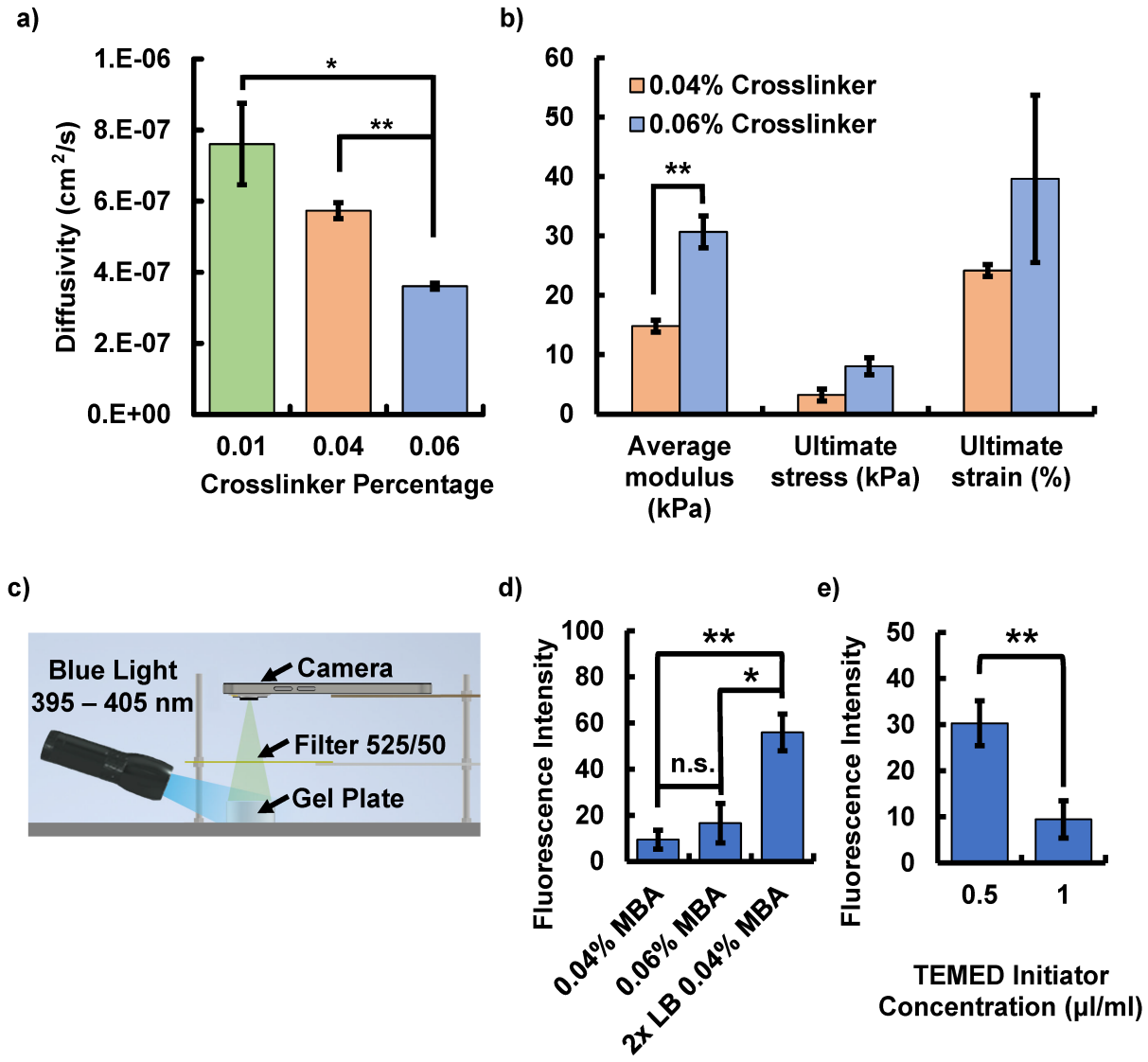

Figure S9: The pAAM nutrient layer was tuned for diffusivity, mechanical properties, and growth. a) Diffusivity significantly decreased when the crosslinker percentage was increased. b) Mechanical properties of pAAM gels with varied crosslinker percentages determined using uniaxial tensile testing. Note that 0.01% crosslinker was not sufficiently stiff for tensile testing. c) Imaging setup consisting of a blue light for excitation and a filter for the GFP emission wavelength to enable full plate imaging for assessment of growth via fluorescence. d) The percentage crosslinker did not significantly alter the growth for the compositions tested while doubling the nutrient concentration did statistically significantly increase growth. e) Bacterial fluorescence for varied TEMED initiator concentrations for the nutrient layer. All error bars report standard error of the mean (n=3).

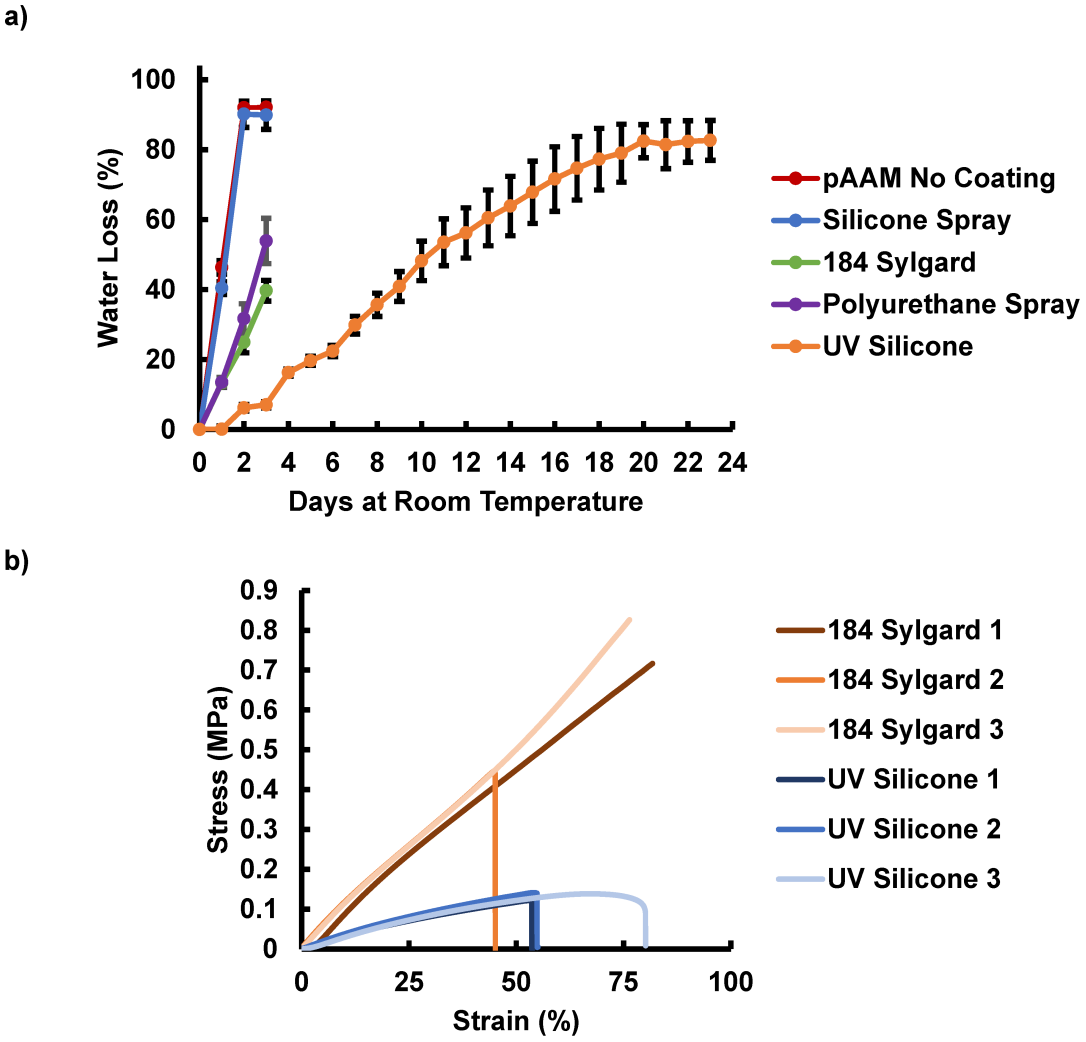

Figure S10: a) Water loss measured via change in gel weight over time for pAAM nutrient gel plates covered with different coatings. Tests were conducted at a temperature of 23°C and 30% humidity. b) Comparison of the mechanical properties of commonly used 184 Sylgard PDMS with UV-cured silicone. All error bars report standard error of the mean (n=3).

Table S2: Summary of mechanical properties obtained from uniaxial tensile testing of 184 Sylgard PDMS and UV Silicone.

Material	**Young's Modulus (GPa)**	**Ultimate Tensile Stress (MPa)**	**Strain to Failure (%)**
184 Sylgard	1.03 ± 0.06	0.80 ± 0.38	81.79 ± 35.08
UV Silicone	0.31 ± 0.02	0.13 ± 0.01	63.00 ± 14.86

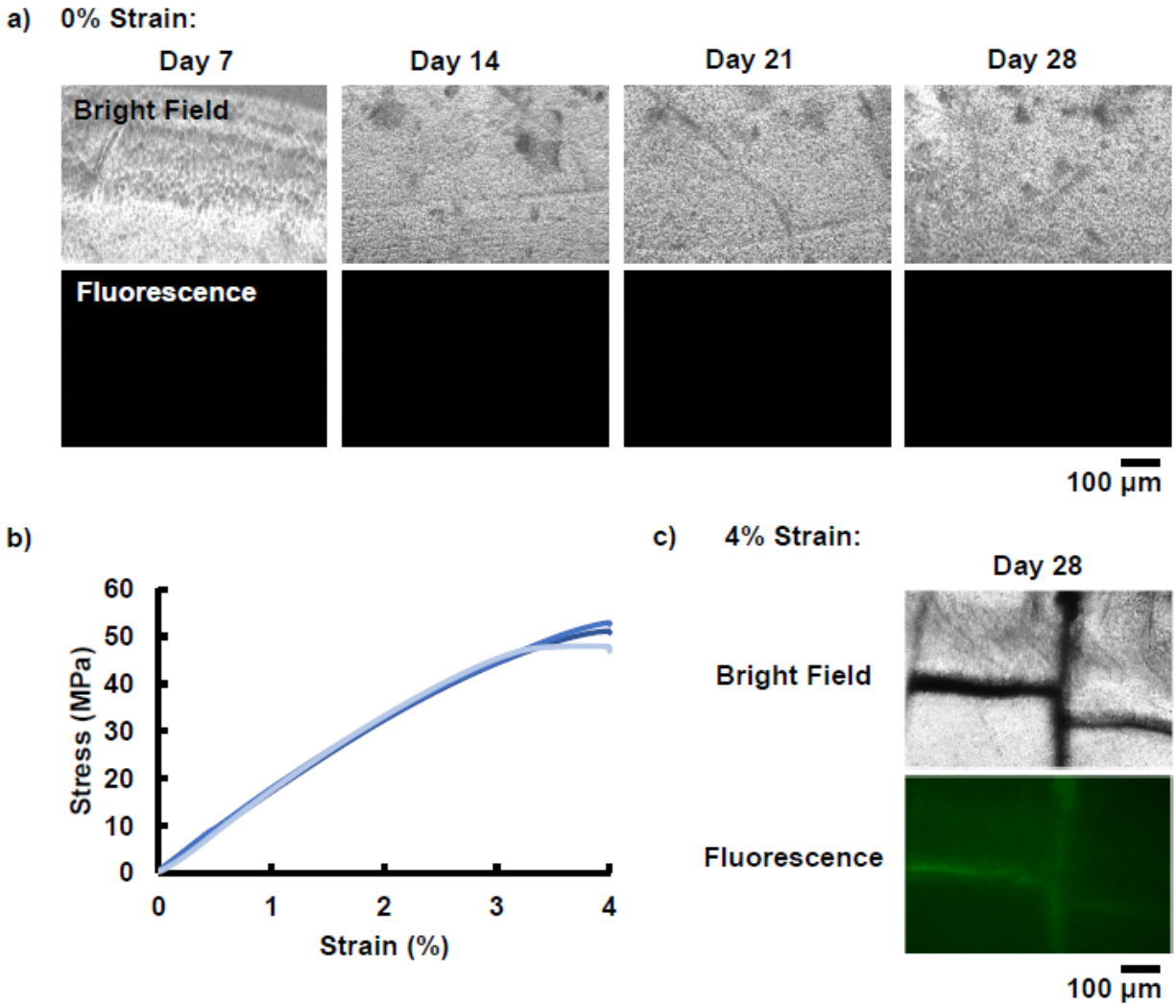

Figure S11: Microscopy images of spore-PMMA coated polycarbonate dog bone samples (with the nutrient and UV-silicone layers) stored for up to 28 days in a humidity chamber at 25°C, 95% humidity. No spontaneous germination or fluorescence was observed. b) At 28 days, three samples were tested to 4% strain and c) imaged after 24 hours of growth demonstrating successful detection after a period of storage.

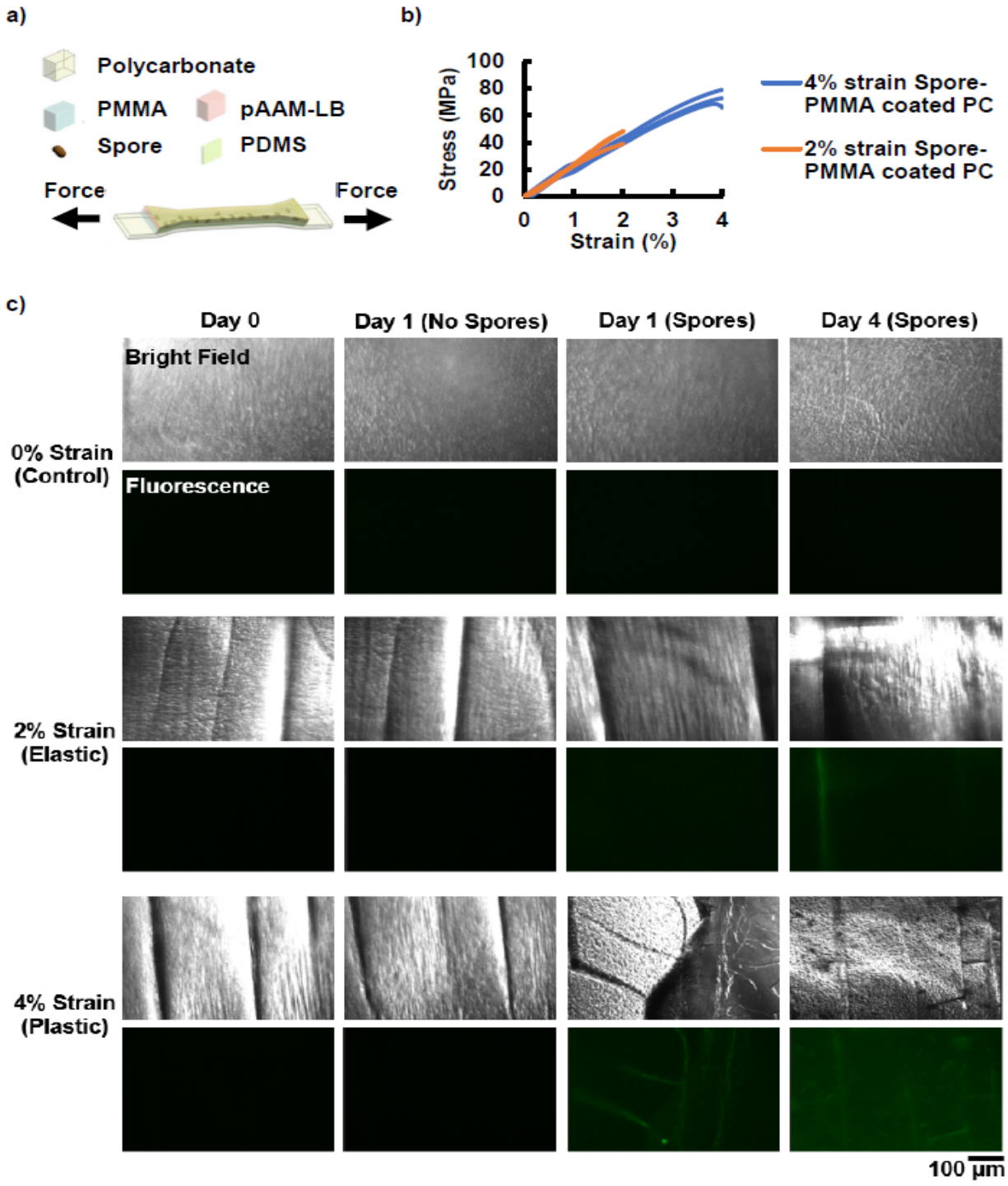

Figure S12: a) Schematic of polycarbonate dog bone sample with spore-PMMA coating, nutrient layer and PDMS layer. b) Stress-strain results for samples tested to 2% strain and 4% strain showing elastic and plastic behavior respectively. c) Microscopy images of samples tested to 0%, 2%, 4% strain. Low signal fluorescent crack detection was observed at Day 4 for 2% strain samples and Day 1 for 4% samples.

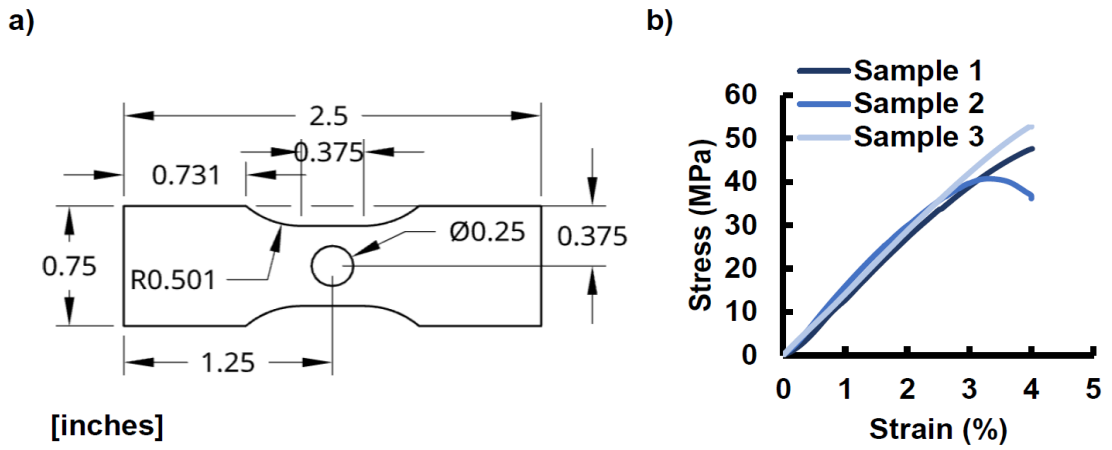

Figure S13: a) Diagram of dog bone dimensions with circular stress concentration. b) Stress-strain curves for three trials for Figure 4a ii for monotonic loading of the complete silicone, pAAM, spore-PMMA coating on PC dog bone samples with a circular stress concentration.

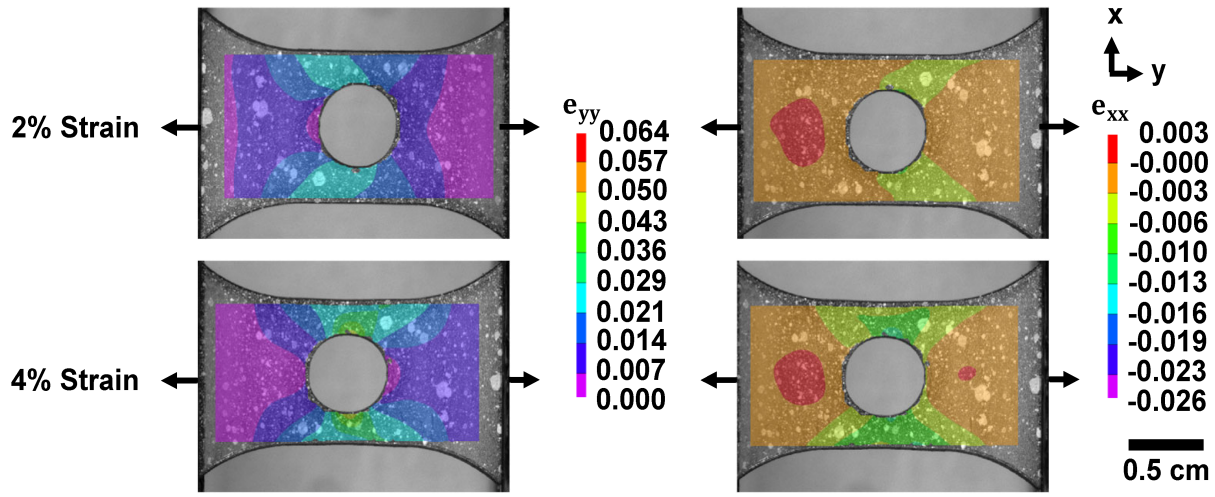

Figure S14: a) Digital image correlation results showing strain contour plots for strains in the y- (e_{yy}) and x-directions (e_{xx}) for polycarbonate spore-PMMA coated samples with 2% and 4% applied strain.

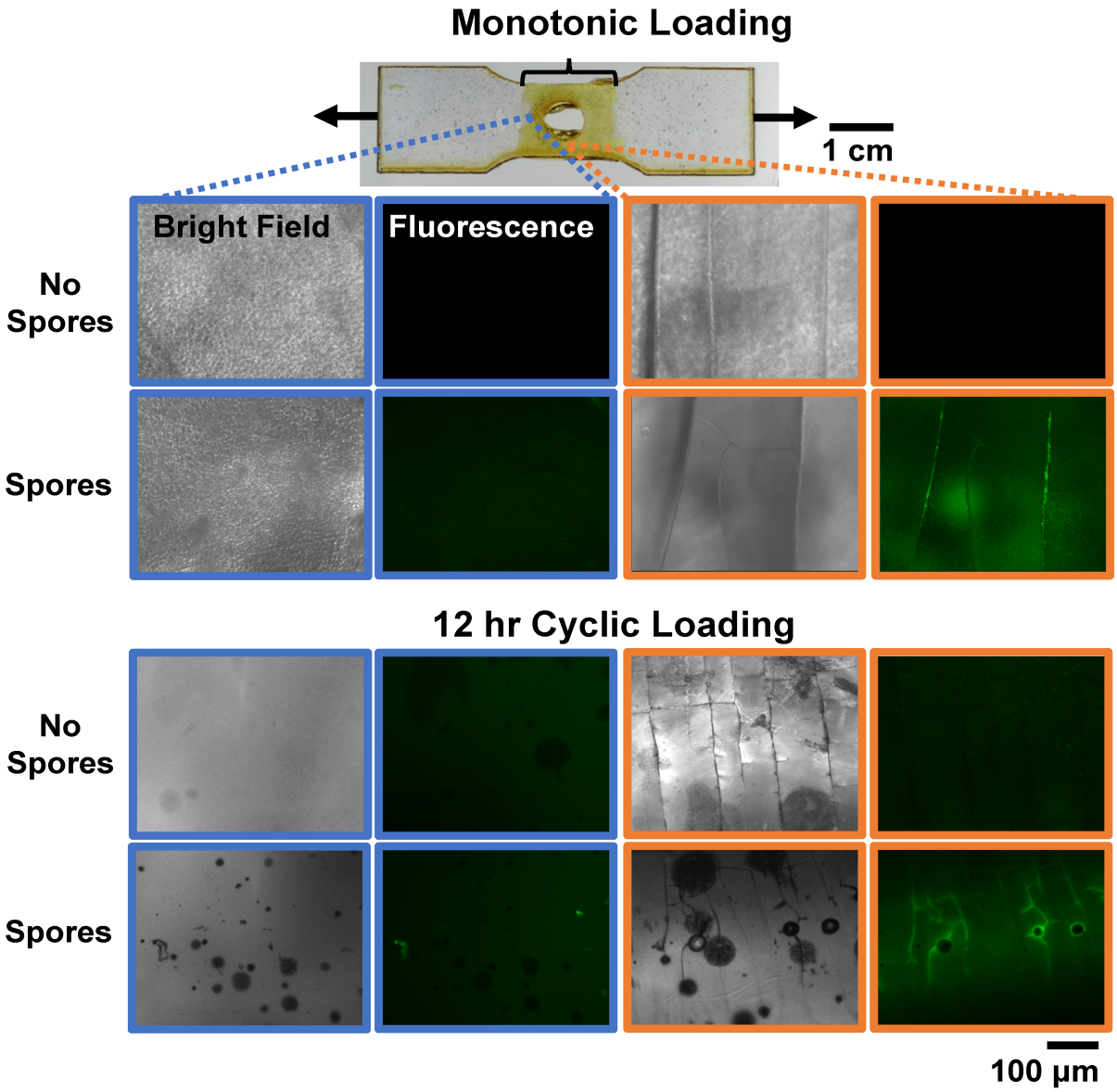

Figure S15: Microscopy images showing the fluorescent crack detection for a sample loaded monotonically to 4% strain and a sample loaded cyclically for 12 hours continuously from 0 to 150 N, at 0.03 Hz and imaged at 12 hours achieving crack detection comparable to the time for bacteria to grow on an LB-agar plate. Dust particles adhered to the sample that remained uncovered for 12 hours.

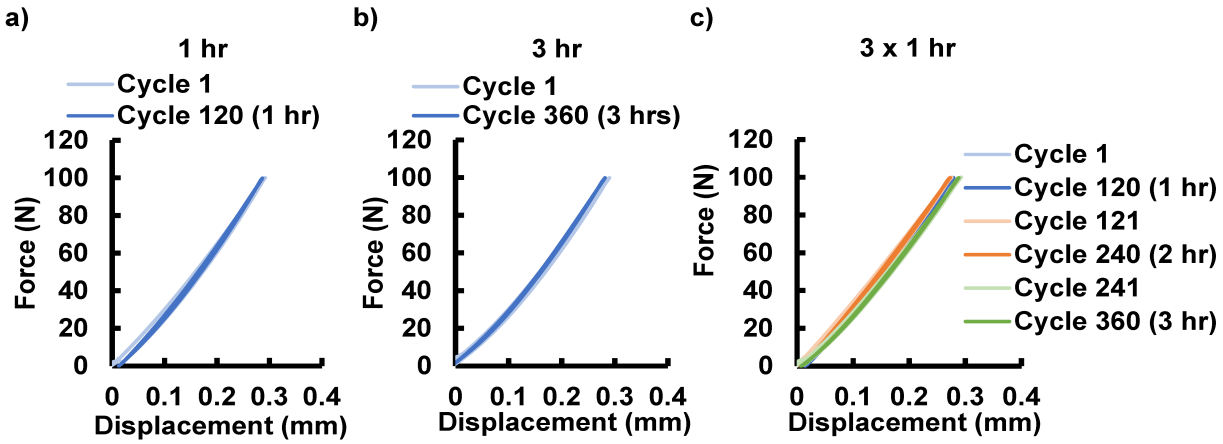

Figure S16: Force-displacement curves for the first and final loading cycles of the fully coated polycarbonate circle stress concentration samples (spore-PMMA, pAAM nutrient gel, and UV-silicone) loaded for a) 1x 1 hour, b) 1x 3 hours, and c) 3x 1 hour.

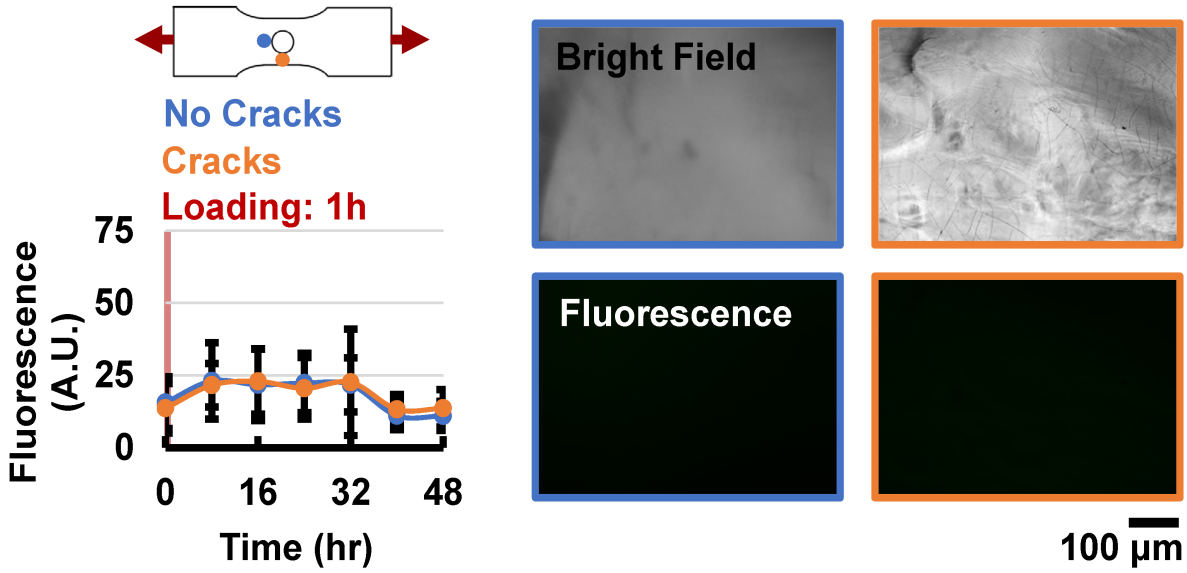

Figure S17: Spore-PMMA coated polycarbonate samples (including the nutrient and silicone layers) loaded for one hour (Figure S16a) did not display any statistically significant fluorescence response via in situ imaging or visible cracks via microscopy.

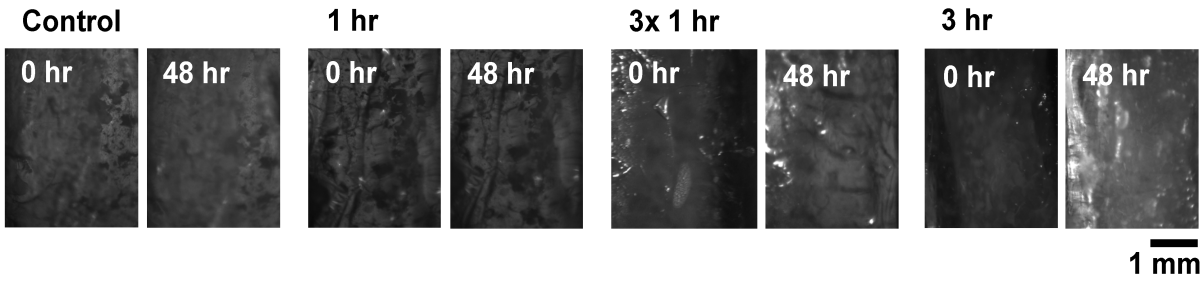

Figure S18: Amplified fluorescence in situ images taken with a grayscale camera for Spore-PMMA coated polycarbonate dog bone samples with circular stress concentrations (including the nutrient and silicone layers) . The images shown were taken at the region of high stress and are scaled from 255 to 127 pixel value brightness scale to enable visual comparison.

5.0 Crack Detection For Polycarbonate and Steel Substrates

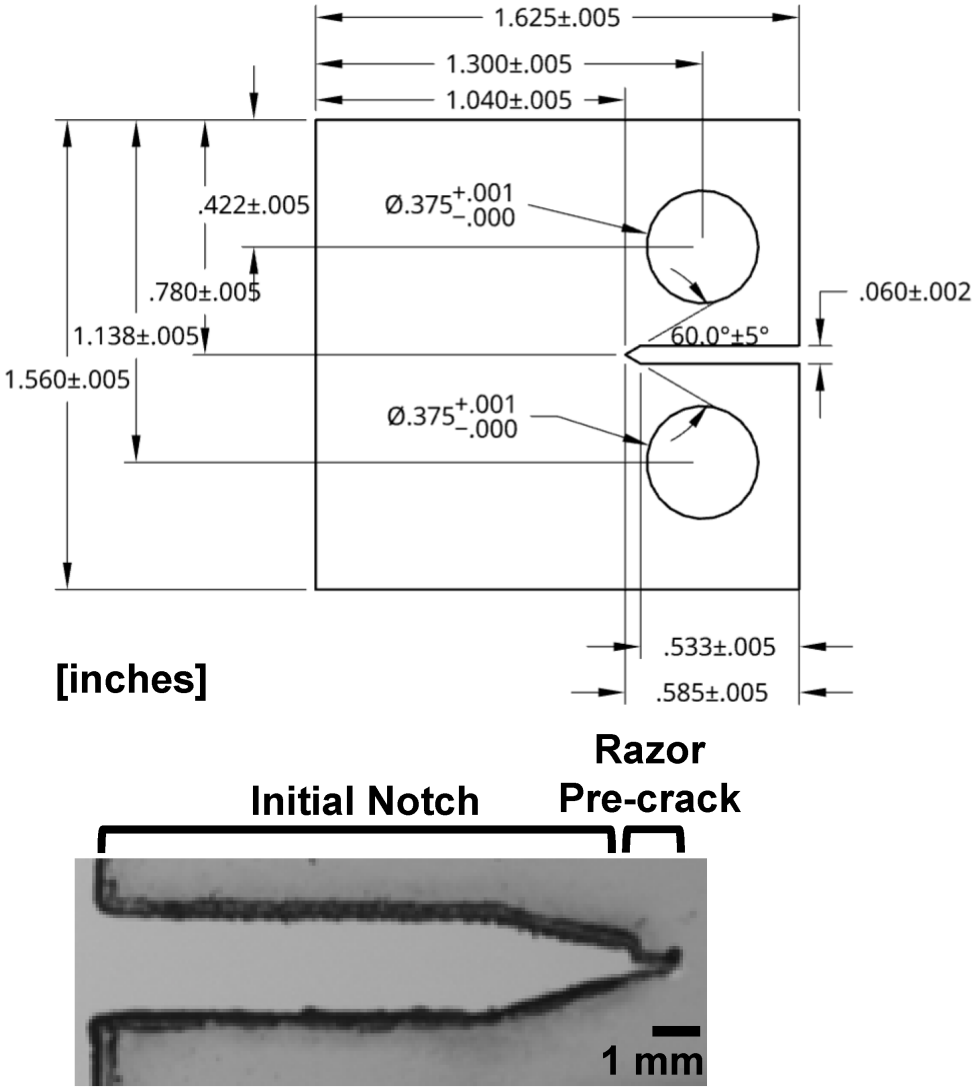

Figure S19: Compact tension testing geometry following ASTM 3999 and image of a polycarbonate compact tension sample with the razor pre-crack.

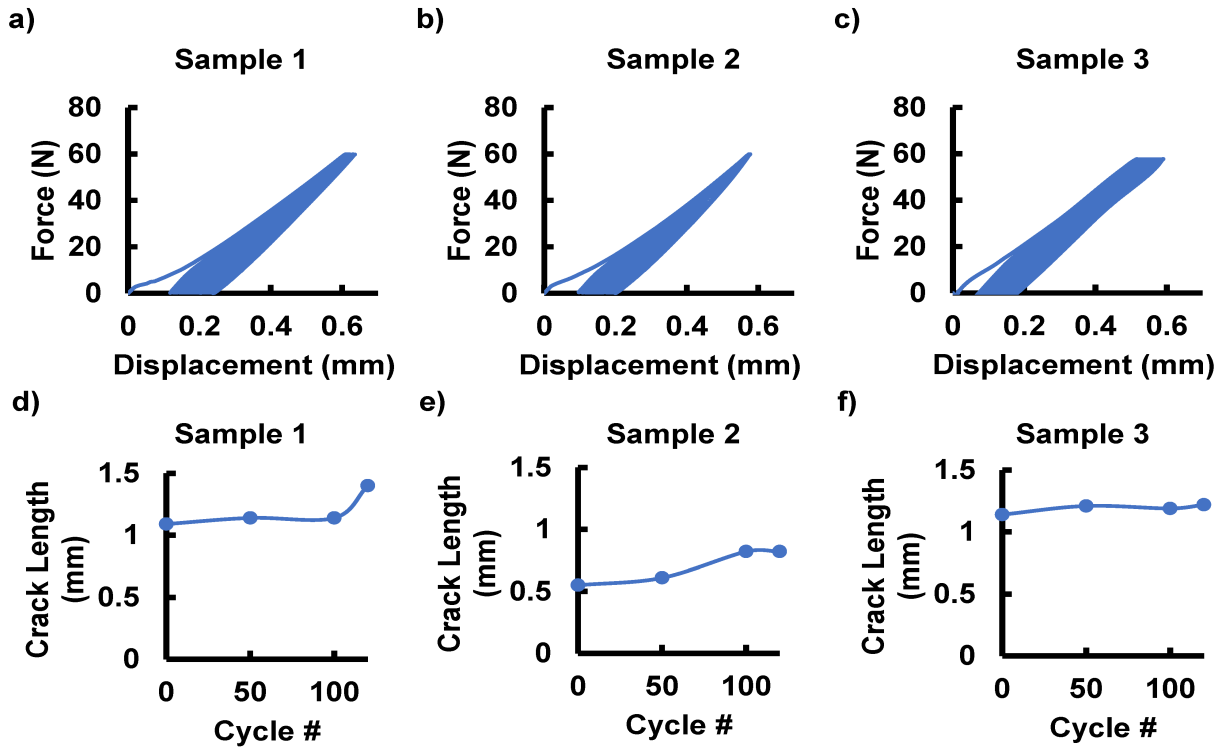

Figure S20: a-c) Force-displacement curves for cyclic loading of three polycarbonate compact tension samples for 1 hour, 0.03 Hz. d-f) Crack growth curves for polycarbonate compact tension test for each of the 3 samples loaded for 1 hour at 0.03 Hz.

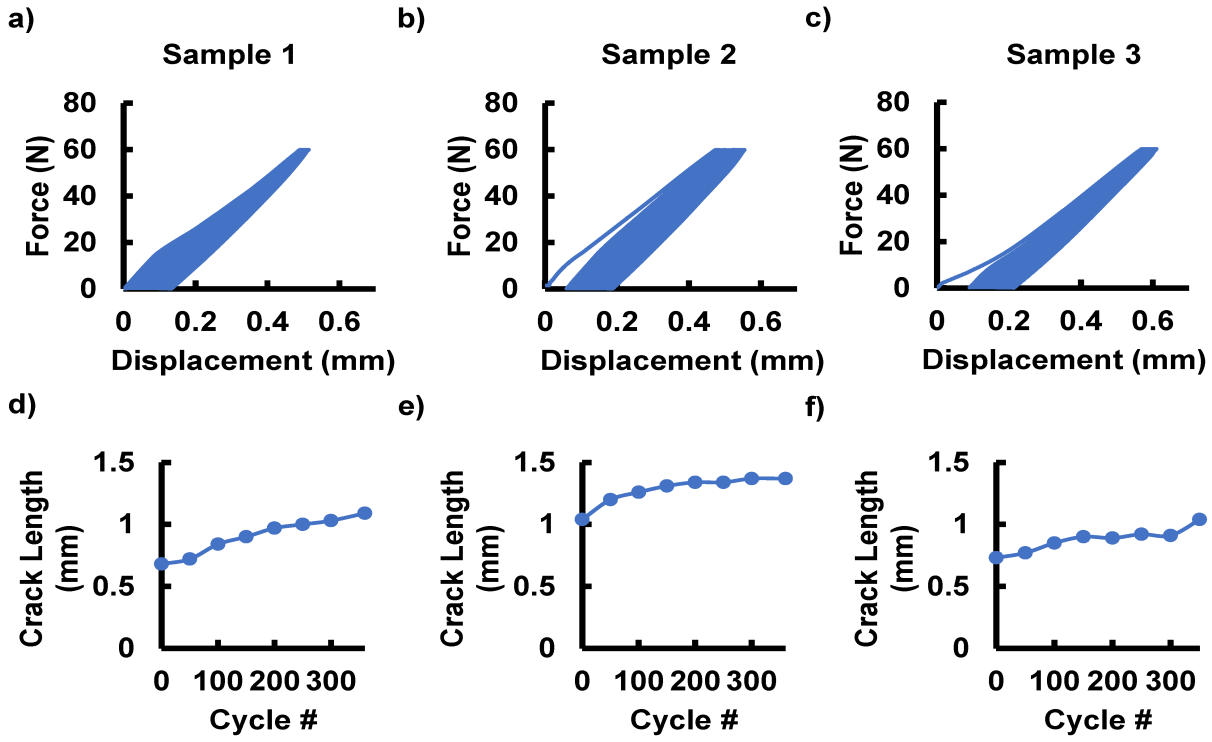

Figure S21: a-c) Force-displacement curves for cyclic loading of three polycarbonate compact tension samples for 3 hours, 0.03 Hz. d-f) Crack growth curves for polycarbonate compact tension test for each of the 3 samples loaded for 3 hours, 0.03 Hz.

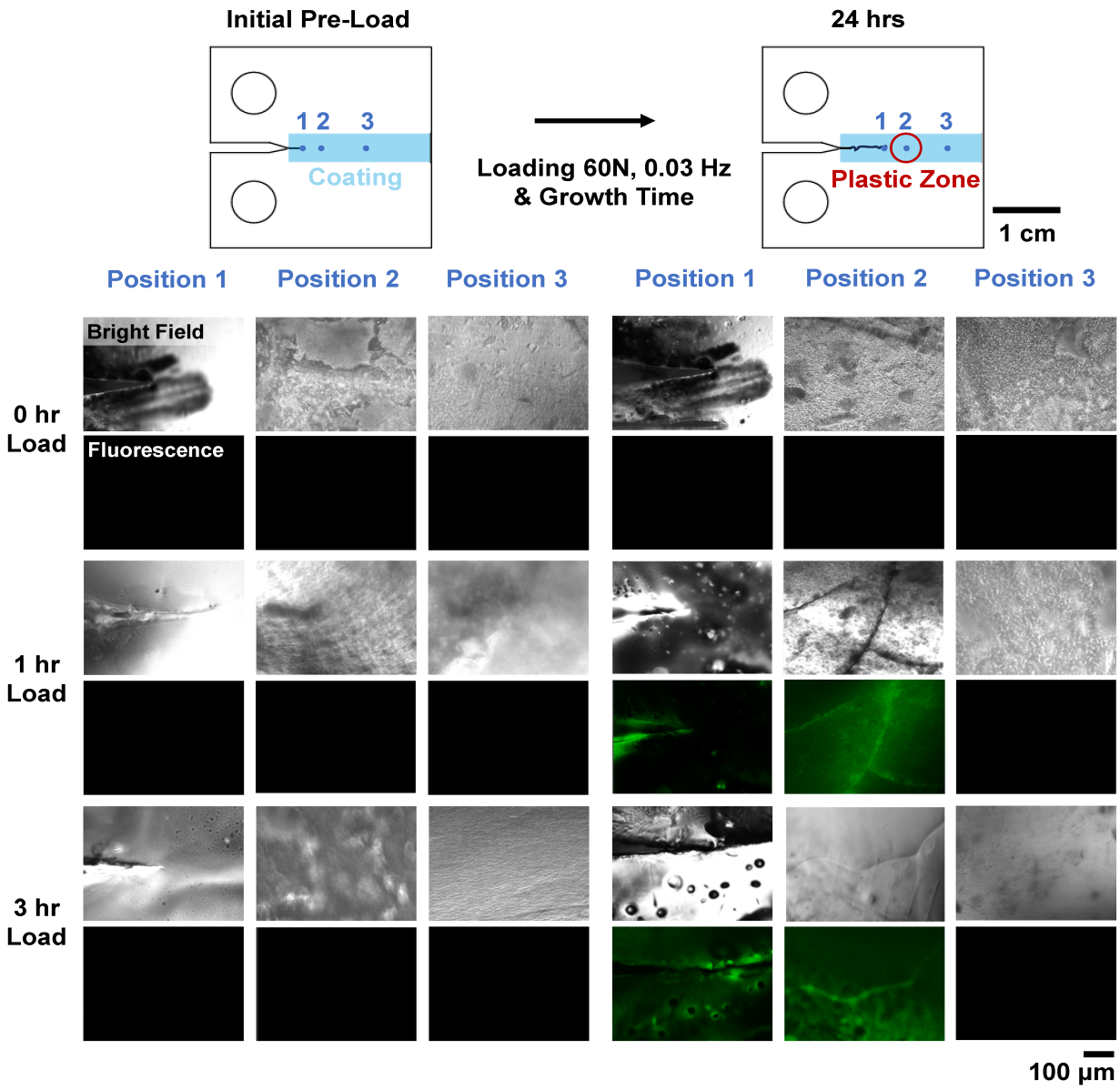

Figure S22: Initial images of polycarbonate compact tension samples taken before loading at each position and for each loading time compared to 24 hour images showing fluorescence response for cracks. Loading was at 60 N, 0.03 Hz.

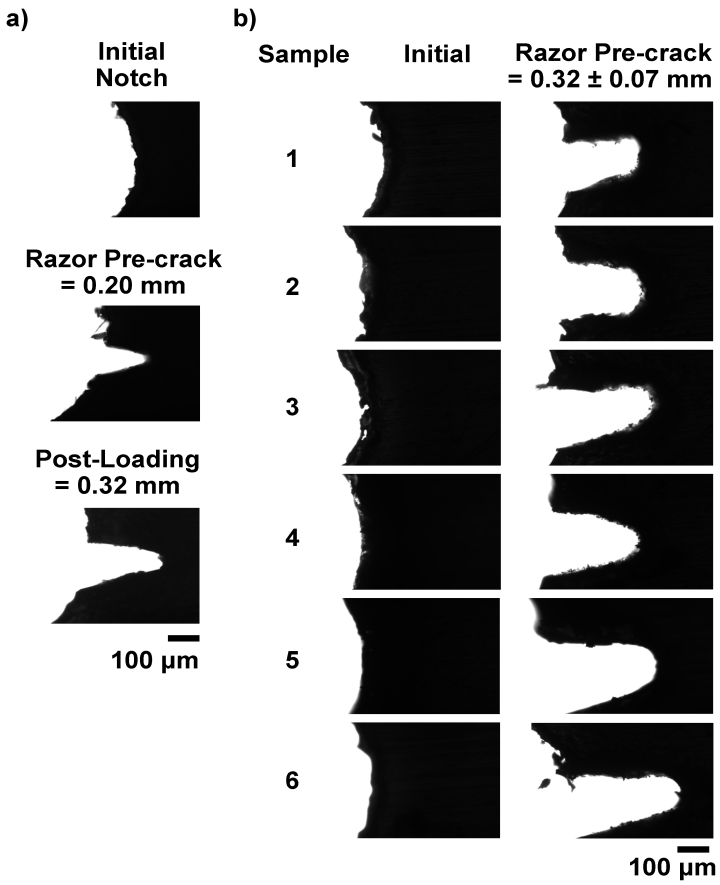

Figure S23: Sample silhouettes for a) an example of an initial notch, razor pre-crack, and post loading for an uncoated steel sample showing crack growth and b) the initial water jet samples and razor pre-crack before coating for all samples tested.

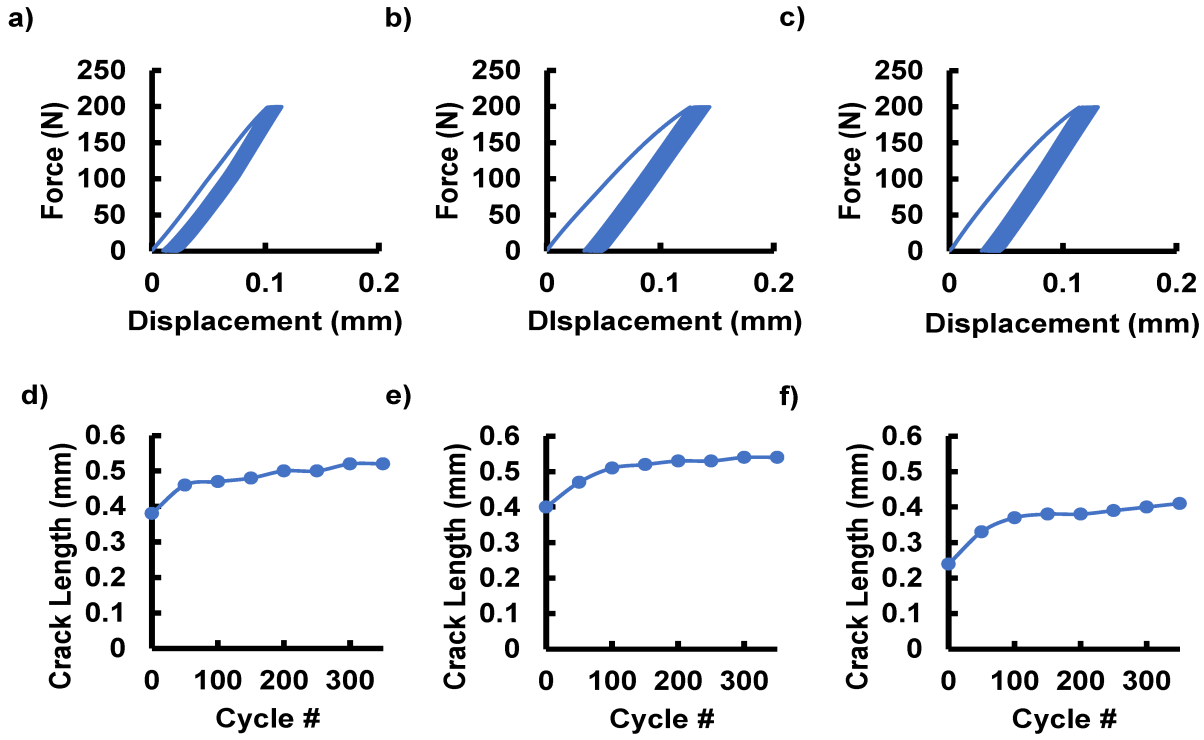

Figure S24: a-c) Force-displacement curves for cyclic loading of three steel compact tension samples for 2 hours 0.05 Hz. d-f) Crack growth curves for steel compact tension test for each of the 3 samples loaded for 2 hours.

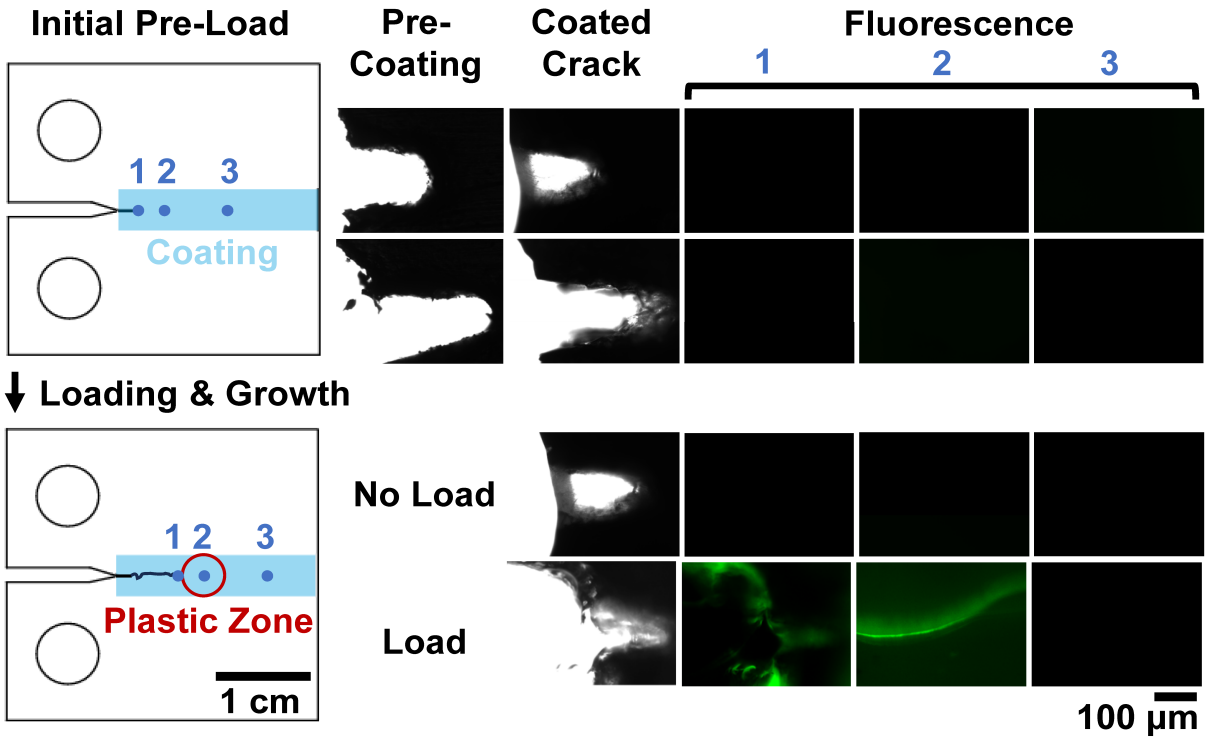

Figure S25: Initial images of steel compact tension samples taken before loading at each position and for each loading time compared to 24 hour images showing fluorescence response for cracks. Loading was for 2 hours, 200 N, 0.05 Hz.

References

[1] M. A. Schaefer, H. N. Nelson, J. L. Butrum, J. R. Gronseth, and J. H. Hines. A low-cost smartphone fluorescence microscope for research, life science education, and STEM outreach. *Sci. Rep.*, 13(1):2722, 2023-03-09.

[2] J. Schindelin, I. Arganda-Carreras, E. Frise, V. Kaynig, M. Longair, T. Pietzsch, S. Preibisch, C. Rueden, S. Saalfeld, B. Schmid, J.-Y. Tinevez, D. J. White, V. Hartenstein, K. Eliceiri, P. Tomancak, and A. Cardona. Fiji: an open-source platform for biological-image analysis. *Nat. Methods*, 9(7):676–682, 2012-07.